ChemistrySelect

Research Article
doi.org/10.1002/slct.202404185

Chemistry Europe
European Chemical Societies Publishing

www.chemistryselect.org

In Silico Identification of Potential Inhibitors for Dengue Virus NS5 Methyltransferase: Molecular Docking, Dynamics, DFT, and ADME Analysis

Bhanuranjan Das,*[a] Purna Chandra Pal,*[b] and Anjali A Upadhyay[c]

Dengue virus (DENV) is a major global health concern, infecting over 100 million people annually with high mortality due to the absence of effective antiviral therapies. The NS5-methyltransferase (NS5-MTase), crucial for DENV replication, is a promising target for drug development. This study investigated phytocompounds as potential NS5-MTase inhibitors. A virtual screening of 25,000 phytocompounds against the S-adenosylmethionine (SAM) binding site identified four promising inhibitors (CNP0014493, CNP0014756, CNP0018882, and CNP0019696) based on docking scores and binding interactions. Molecular dynamics (MD) simulations, confirmed the stablity of these inhibitor complexes under physiological conditions, with free energy landscape analysis further supporting their thermodynamic stability. Density functional theory (DFT) study revealed that CNP0019696 and the reference compound exhibited favorable electronic properties for strong binding interactions. Additionally, in silico ADME (absorption, distribution, metabolism, and excretion) analysis suggested favorable physicochemical properties, indicating good drug-like characteristics and bioavailability. Among the candidates, CNP0014493 and CNP0014756 emerged as the most promising, demonstrating significant potential as therapeutic agents for dengue treatment. These findings underscore the importance of targeting NS5-MTase in developing effective antiviral therapies and highlight the potential of phytocompounds in contributing to the global fight against DENG.

1. Introduction

Dengue fever, a mosquito-borne viral infection caused by the dengue virus (DENV), represents a significant global health concern. According to the World Health Organization (WHO), over 100 million people worldwide contract dengue fever each year, with a substantial number of cases resulting in severe disease and fatalities.[1,2] The primary vectors responsible for the transmission of DENV are the *Aedes aegypti* and *Aedes albopictus* mosquitoes, which are prevalent in tropical and subtropical regions.[3] Dengue virus comprises four distinct serotypes, namely, DENV1, DENV2, DENV3, and DENV4. Infection with one serotype provides lifelong immunity against that serotype but only partial and temporary cross-immunity against the others.[4] Consequently, individuals can be infected with dengue up to four times in their lifetime, with subsequent infections often leading to more severe forms of the disease, such as dengue hemorrhagic fever (DHF) and dengue shock syndrome (DSS).

Despite the high burden of disease, there are currently no specific antiviral treatments available for dengue infection.[5] The management of dengue primarily focuses on symptomatic relief and supportive care, including the use of analgesics, fluid replacement, and platelet transfusions in severe cases.[6] The lack of targeted therapies underscores the urgent need for research and development of effective antiviral agents and vaccines.[7] Numerous studies are underway to better understand the molecular biology of the dengue virus and identify potential therapeutic targets. One area of active research is the role of the non-structural protein 5 (NS5), which possesses both RNA-dependent RNA polymerase and methyltransferase activities essential for viral replication and survival. Inhibiting the methyltransferase activity of NS5, for instance, represents a promising strategy for antiviral drug development. Furthermore, efforts are being made to develop vaccines that can provide broad and long-lasting protection against all four dengue serotypes.[8]

Recent advancements in our understanding of the dengue virus lifecycle and host-pathogen interactions have paved the way for innovative approaches to combat the disease.[9] However, the complexity of the virus and its interaction with the human immune system poses significant challenges. Continued research and collaboration among scientists, healthcare professionals, and policymakers are crucial to developing effective interventions and ultimately reducing the global burden of dengue fever.

Dengue virus has four serotypes named DENV1–4.[10] The dengue virus genome consists of an 11 kb ss RNA (+) contain-

[a] *B. Das*
Department of Pharmaceutical Engineering & Technology, Indian Institute of Technology (BHU), Varanasi, Uttar Pradesh 221005, India
E-mail: bhanuranjandas.rs.phe20@itbhu.ac.in

[b] *P. C. Pal*
Department of Pharmaceutical Technology, Brainware University, Kolkata, West Bengal 700125, India
E-mail: purnachandrapal11@gmail.com

[c] *A. A Upadhyay*
Lucknow University, Babuganj, Hasanganj, Lucknow, Uttar Pradesh 226007, India

Supporting information for this article is available on the WWW under https://doi.org/10.1002/slct.202404185

ing one large open reading frame encoding a single polyprotein, which is cleaved during and immediately after translation by cellular and a virally encoded protease.[11] Dengue virus genome is a (+) ss RNA coding for 10 proteins of which three are structural proteins (capsid, membrane, and envelope) and seven are nonstructural proteins. These nonstructural proteins are sequentially arranged as NS1-NS2A-NS2B-NS3-NS4A-NS4B-NS5.[12,13] The NS5 consists of a C-terminus RNA dependent-RNA polymerase and an N-terminus methyltransferase (MTase) domain. The (+) RNA genome of flavivirus contains a 5′ terminal cap-1 structure (GpppA-RNA). The MTase subsequently methylates this cap at the N7 position of the guanine and the ribose 2′-OH of the first replicated nucleotide as well as internal adenosines. The action of the NS5-MTase produces methylated cap mGpppA-RNA bringing close 2′-O and N-7 methylation activity is essential for the life cycle of flaviviruses, and hence, methyltransferase represents a novel target for flavivirus therapy.[14] The methyl donor for these reactions is S-adenosyl-L-methionine (SAM), which becomes S-adenosyl-L homocysteine (SAH) as a by-product of the methylation reaction. SAM binding site are mor preferable against DENV MTase because finding a ligand that fixes at the RNA cap site would be a difficult challenge due to the nature of shallow and easily exposed to solvent.[15] Presently there is no effective targeted treatment for dengue. Medicines that are currently available are mainly for symptomatic treatment in terms of painkillers and the infusion of platelets into the body from outside and intake of plenty of fluid.

In this study, we employed virtual screening approaches to identify potential inhibitors of the dengue virus (DENV) NS5 methyltransferase (MTase). The MTase domain of DENV possesses two binding sites: The S-adenosylmethionine (SAM) binding site and the RNA binding site. Due to the shallow and solvent-exposed nature of the RNA cap site, it presents significant challenges for ligand binding. Consequently, the SAM binding site was targeted as a more viable option for inhibiting DENV MTase. We selected the top four molecules based on their binding interactions and docking scores. To gain deeper insights into their binding patterns and stability, molecular dynamics simulations were performed on these four molecules. Free energy landscape analysis further supported the thermodynamic stability of the protein–ligand complexes. Further, DFT study revealed that the reference compound, as well as the top identified ligand CNP0019696, displayed promising stability and electronic properties favorable for binding interactions. Additionally, in silico ADME (absorption, distribution, metabolism, and excretion) studies were conducted to evaluate the pharmacokinetic parameters of the top four ligands. The overall work is summarized in Figure 1.

2. Results and Discussions

2.1. Molecular Docking Study

Firstly 25,000 molecules were downloaded from Coconut database for screening against NS5 MTase SAM binding site of DENV protein.[16] Before screening a molecular docking, study was performed using PyRx for cocrystal ligand sinefungin (SNG), which was selected as reference compound against DENV-3 NS5 MTase (PDB ID: 4R8S) in the SAM binding pocket.[17] SNG was selected as the reference compound for the SAM binding pocket due to its structural similarity to S-adenosyl-L-methionine (SAM), allowing it to mimic SAM's interactions and act as a competitive inhibitor. SNG is well-characterized and widely used in studies of SAM-dependent methyltransferases, making it a reliable reference for evaluating new inhibitors. Its effectiveness across multiple methyltransferases further supports its use in our study.[18,19] Dock RMSD (root-mean-square deviation) SNG between cocrystal and after docking was 1.47 Å (Figure S1B, Supporting Information), which indicate that the docking parameter are correct.[20] The docking interaction analysis of SNG with DENV-3 NS5 MTase domain showed strong binding affinity (−8.8 kcal/mol) with several hydrogen bonds with residues Ser56, Thr104, Lys105, and His110 and hydrophobic interaction with Arg84, Val 132, Ile147 residues (Figure S1A). All the 25,000 molecules were screened using same protocol as used in case of reference compound SNG using PyRx. We selected 38 molecules on the basis of higher binding energy (Kcal/mol) than reference compound (−8.8 kcal/mol) (Table S1, Supporting Information). Finally, we selected 4 molecules based on standard interaction (Ser56, Gly86, Trp87, Asp131, Asp146, His110, Val132, Lys105) and structural similarity with reference compound (Table S2). Figure 2 shows the structure of standard compound and best selected top scoring hit molecules.

Analysis of docked pose of CNP0014493 at SAM binding site of DENV NS5-MTase (Figure 3a,b) showed strong binding affinity (−10.1 kcal/mol), and it formed several hydrogens bonds with protein residues like Ser56, Gly86, Thr104, Lys105, Val132 as well as several hydrophobic interactions noted with residues like Gly83, Arg84, Trp87, Ile147. A H bond was observed between oxygen atom of piperonyl ring of the compound CNP0014493 and OH side chain of Ser56, as well as NH backbone of Gly86 of protein. Another H bond formed between amine group of pyrimidazole and NH2 backbone of Thr104 and NH2 backbone Lys105 amino acid residue of protein. Another H bond was formed between N atom of pyrimidazole ring of the compound CNP0014493 and NH2 group of Val132. Compound CNP0014493 not only formed H bond but also formed several hydrophobic interactions like π–alkyl between piperonyl ring (—CH2) methylene group and Trp87 amino acid residue of protein. Additionally, hydrophobic (π–π) interactions between piperonyl ring and Gly83 and Arg84 and between pyrimidazole ring and Ile147 were observed.

Analysis of docked pose of CNP0014756 at SAM binding site of DENV NS5-MTase (Figure 3c,d) showed good binding affinity (−9.5 kcal/mol), and it formed several hydrogens bonds with protein residues like Ser56, Lys105 as well as several hydrophobic interactions noted with residues like Gly81, Arg84, Val132, Asp146, Ile147. One H bond formed between N atom of pyrimidine ring of the molecule and side chain OH group of Ser56 amino acid residue of protein. Another H bond formed between N atom of benzimidazole ring of the molecule and NH backbone of Lys105 amino acid residue of protein. π–π hydrophobic interaction between benzimidazole ring and Val132, Ile147 amino

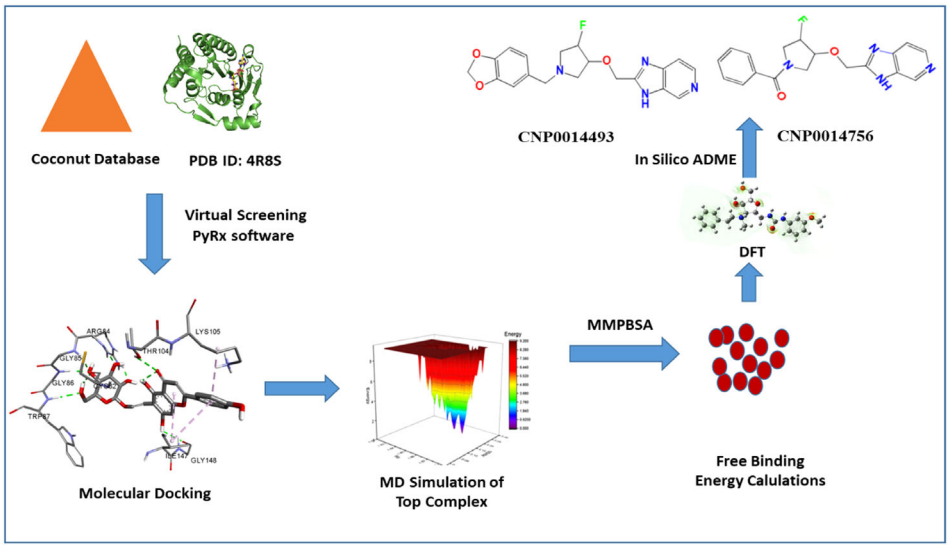

Figure 1. Schematic representation of the workflow used to identify active ligands. Structure-based virtual screening of 25,000 natural ligands from the Coconut database was performed using PyRx software. Four molecules were selected from the top 38 based on their binding patterns. Further molecular dynamics and binding free energy study revealed the stability of the complex.

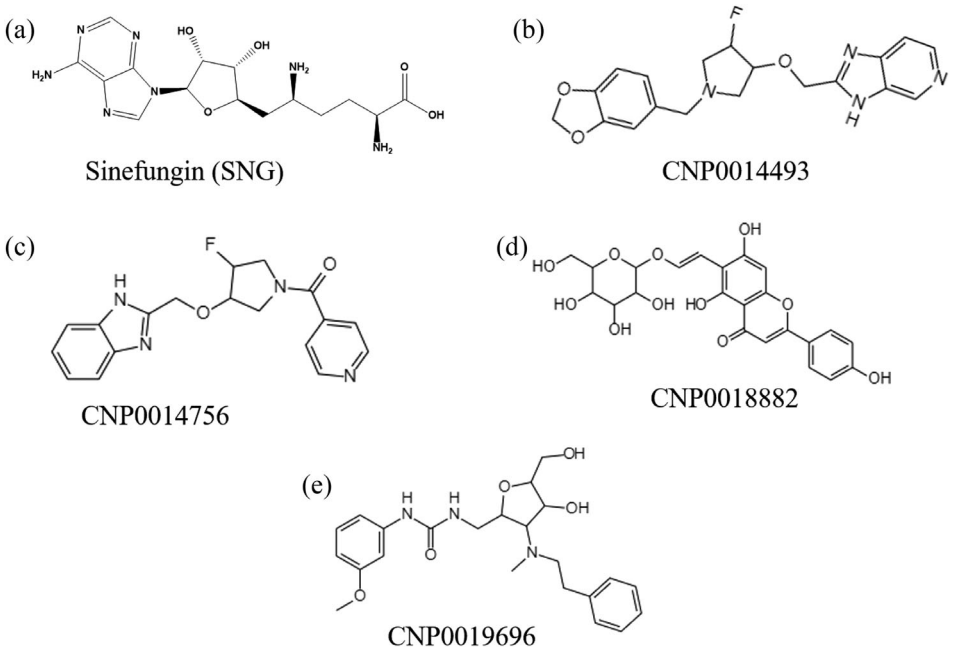

Figure 2. Standard inhibitor and best selected compounds from coconut database against dengue virus NS5 methyltransferase: (a) sinefungin (SNG), (b) CNP0014493, (c) CNP0014756, (d) CNP001882, and (e) CNP0019696, respectively.

acid residue of protein was observed. Another $\pi-\pi$ interaction between pyrimidine ring and Arg84 amino acid residue of protein was observed. Two halogen interaction between fluorine atom of pyrrolidine ring and Gly81, Asp146 amino acid residues was detected.

Analysis of docked pose of CNP0018882 at SAM binding site of DENV NS5-MTase (Figure 4a,b) showed good binding affinity (−10.7 kcal/mol), and it formed several hydrogens bonds with protein residues like Cys82, Arg84, Gly85, Gly86, Trp87, Thr104, Gly148 as well as several hydrophobic interactions noted with residues like Lys105, Ile147. CNP0018882 is a flavonoid glucoside, forming H bond between (—C═O) ketone group of flavonoid glucosides and side chain OH group of Thr104 amino acid residue of protein. Another H bond between 7 positions OH group of flavonoid and acid (—C═O) backbone of amino acid residue Gly148.

The molecular docking analysis of CNP0019696 revealed several interactions with the DENV NS5-MTase protein (Figure 4c,d). The oxygen atom showed hydrogen bond interactions with different residues like Ser56, Gly83 Glu111. π–cation hydrophobic interaction between phenyl ring of compound CNP0019696 and Lys105 amino acid residue of protein was formed. Another $\pi-\pi$

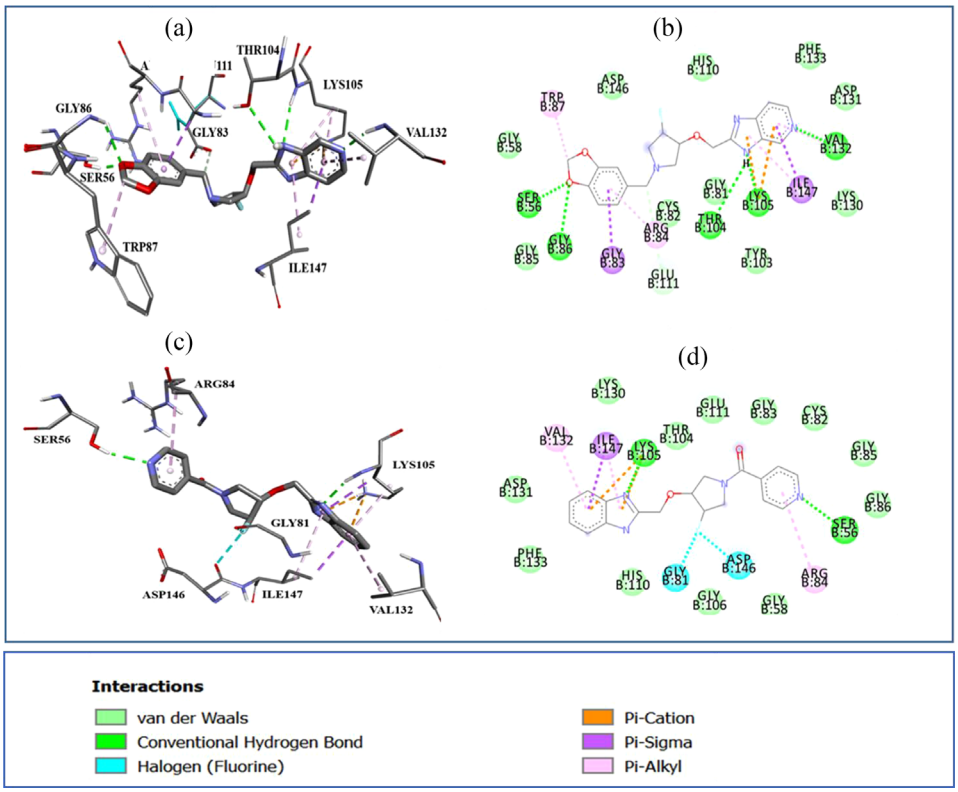

Figure 3. Results of docking of target proteins NS5-MTase (PDB ID-4R8S) with different ligands in 3-D and 2-D respectively for (a,b) CNP0014493 and (c,d) CNP0014756. The different types of interactions are shown by different colors mentioned in the interactions panel. The interactions were visualized and analyzed using Biovia Discovery studio client 2020.

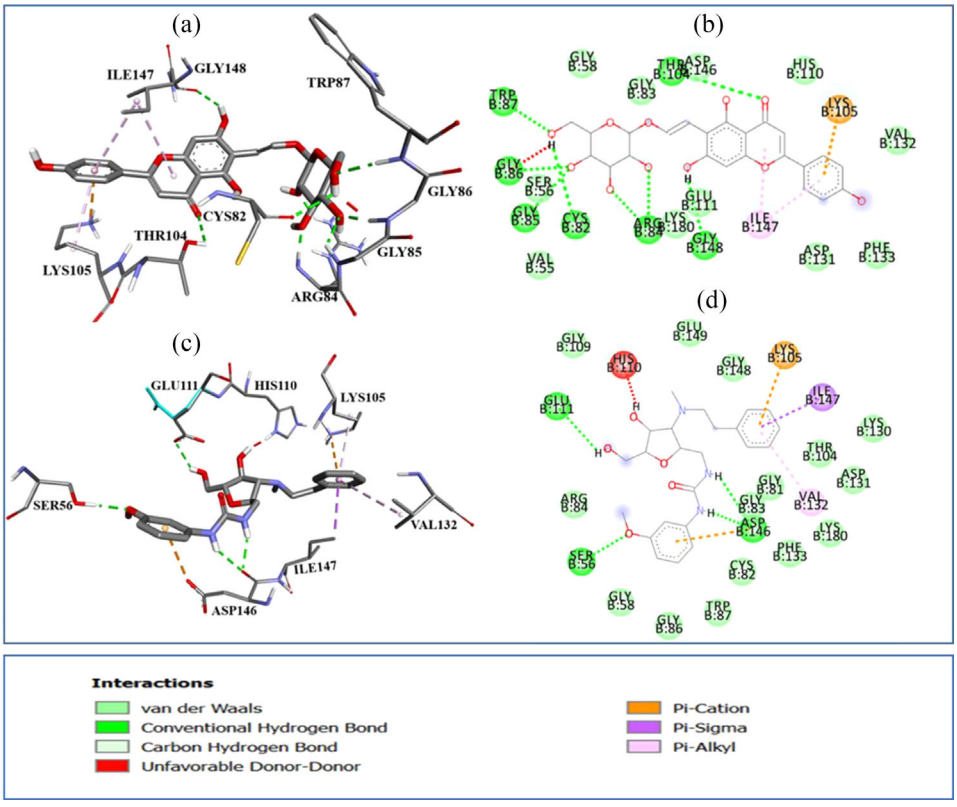

Figure 4. Results of docking of target proteins NS5-MTase (PDB ID-4R8S) with different ligands in 3-D and 2-D respectively for (a,b) CNP0018882 and (c,d) CNP0019696. The different types of interactions are shown by different colors mentioned in the interactions panel. The interactions were visualized and analyzed using Biovia Discovery studio client 2020.

interaction between phenyl ring of compound CNP0019696 and amino acid residue Ile147, Val132 was formed.

2.2. Molecular Dynamics Simulation

To better comprehend the interaction and stability of the ligands with 4R8S protein residues, molecular dynamic simulation study was performed for 100 ns by using GROMACS software. The MD analysis of all four complex were discussed below.

2.2.1. Molecular Dynamics Simulation of lig_CNP0014493-4R8S Complex

Root-mean-square deviation (RMSD) is a common metric used in molecular dynamics simulations to quantify the deviation of a set of coordinates from a reference structure. It provides a measure of the overall structural similarity or dissimilarity between different snapshots of a molecular system during a CNP0014493 simulation. The RMSD of the dengue virus protein (Figure 5a) fluctuates between 0.10 and 0.25 nm initially flapping for 40 ns and remains stable for rest simulation. RMSD of lig_CNP0014493 showed fluctuation more initially for 60 ns and then stable for rest of the simulation. The RMSF values for certain ligand atoms range from 0.2 to 0.35 nm, reflecting their flexibility and the efforts they exert in interacting with protein atoms (Figure 5b). Additionally, the RMSF of specific amino acids—namely residues 50, 100, 355, and 250—shows higher fluctuations (0.25–0.35 nm), indicating that these residues are notably more flexible than others (Figure 5c). The radius of gyration (R_g) for the complex lig_CNP0014493-4R8S remained consistent throughout the simulation period, suggesting the complex's stability (Figure 5d).

In addition, we performed an assessment of hydrogen bond distributions to delve deeper into the system's stability. As depicted in Figure 6a,b, the molecule displayed a significant number of hydrogen bond distributions over the entire 100 ns duration, using a cutoff value of 0.35 nm. This finding highlights the heightened stability of the system, suggesting a persistent presence and maintenance of intermolecular interactions involving hydrogen bonding throughout the simulation.

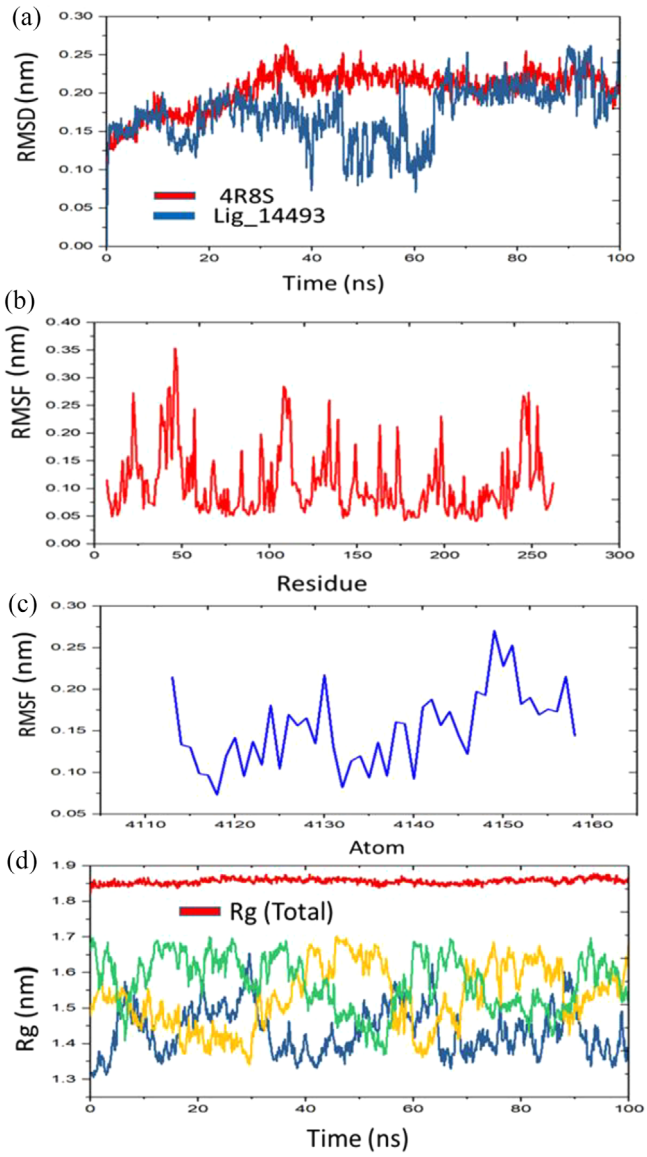

Figure 5. Molecular dynamics trajectory analysis of compound lig_14493_4R8S complex. (a) RMSD, (b) RMSF of protein, (c) RMSF of ligand, and (d) R_g of the complex.

2.2.2. Molecular Dynamics Simulation of lig_CNP0014756-4R8S Complex

The RMSD analysis of the dengue protein 4R8S, illustrated in Figure 7a, reveals a fluctuation range from 0.2 to 0.8 nm. Notably, there is an initial heightened fluctuation during the first 40 ns, after which the RMSD stabilizes for the remainder of the simulation period. Concurrently, the RMSD of the ligand maintains stability, ranging between 0.02 and 0.2 nm throughout the entire simulation. Examining the root-mean-square fluctuation (RMSF) of the protein (Figure 7b), fluctuations in the range of 0.05 to 0.25 nm are observed for residues 50, 100, 150, 200, and 250. This variability in RMSF underscores the flexibility of these specific residues, indicative of dynamic interactions with ligand atoms. Similarly, the RMSF of the ligand (Figure 7c) demonstrates fluctuations between 0.05 and 0.20 nm, illustrating the ligand's flexibility in interacting with protein residues. Furthermore, the radius of gyration (R_g) analysis of the complex, as depicted in Figure 7d, indicates a consistent stability of the complex throughout the simulation. These collective findings provide valuable insights into the dynamic behavior, stability, and intermolecular interactions within the studied dengue protein–ligand complex.

In addition, we performed an assessment of hydrogen bond distributions to delve deeper into the system's stability. As depicted in Figure 8a,b, the molecule displayed a significant number of hydrogen bond distributions over the entire 100 ns duration, using a cutoff value of 0.35 nm. This finding highlights the heightened stability of the system, suggesting a persistent presence and maintenance of intermolecular interactions involving hydro bonding throughout the simulation.

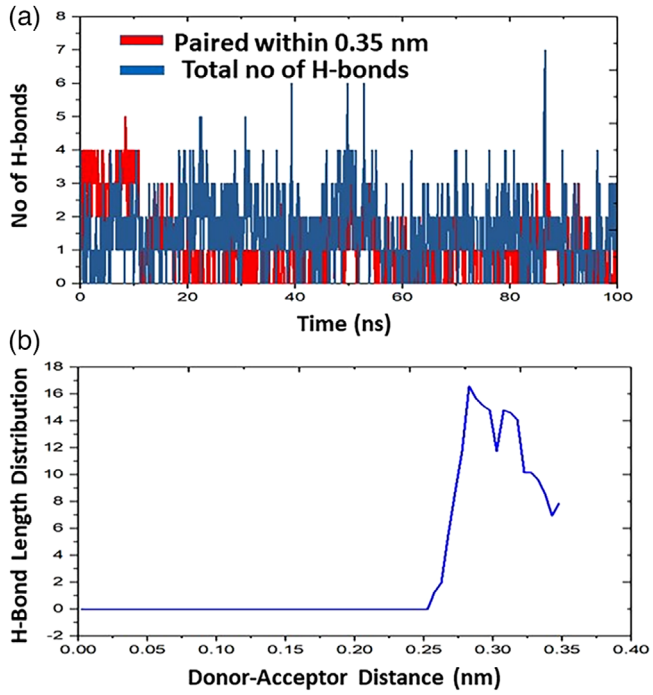

Figure 6. Hydrogen bond trajectory analysis of lig_14493_4R8S complex. (a) Total number of H bonds and (b) H bond length distributions.

2.2.3. Molecular Dynamics Simulation of lig_CNP0018882-4R8S Complex

The RMSD analysis of the dengue protein 4R8S, illustrated in Figure 9a, reveals a fluctuation range from 0.05 to 0.3 nm. Notably, there is an initial heightened fluctuation during the first 20 ns, after which the RMSD stabilizes for the remainder of the simulation period. Concurrently, the RMSD of the ligand maintains stability, ranging between 0.02 and 0.2 nm throughout the entire simulation. Examining the RMSF of the protein (Figure 9b), fluctuations in the range of 0.05–0.25 nm are observed for residues 50, 100, 150, 200, and 250. This variability in RMSF underscores the flexibility of these specific residues, indicative of dynamic interactions with ligand atoms. Similarly, the RMSF of the ligand (Figure 9c) demonstrates fluctuations between 0.01 and 0.07 nm, illustrating the ligand's flexibility in interacting with protein residues. Furthermore, the R_g analysis of the complex, as depicted in Figure 9d, indicates a consistent stability of the complex throughout the simulation. These collective findings provide valuable insights into the dynamic behavior, stability, and intermolecular interactions within the studied dengue protein–ligand complex.

In addition, we performed an assessment of hydrogen bond distributions to delve deeper into the system's stability. As depicted in Figure 10a,b, the molecule displayed a significant number of hydrogen bond distributions over the entire 100 ns duration, using a cut-off value of 0.35 nm. This finding highlights the heightened stability of the system, suggesting a persistent presence and maintenance of intermolecular interactions involving hydrogen bonding throughout the simulation.

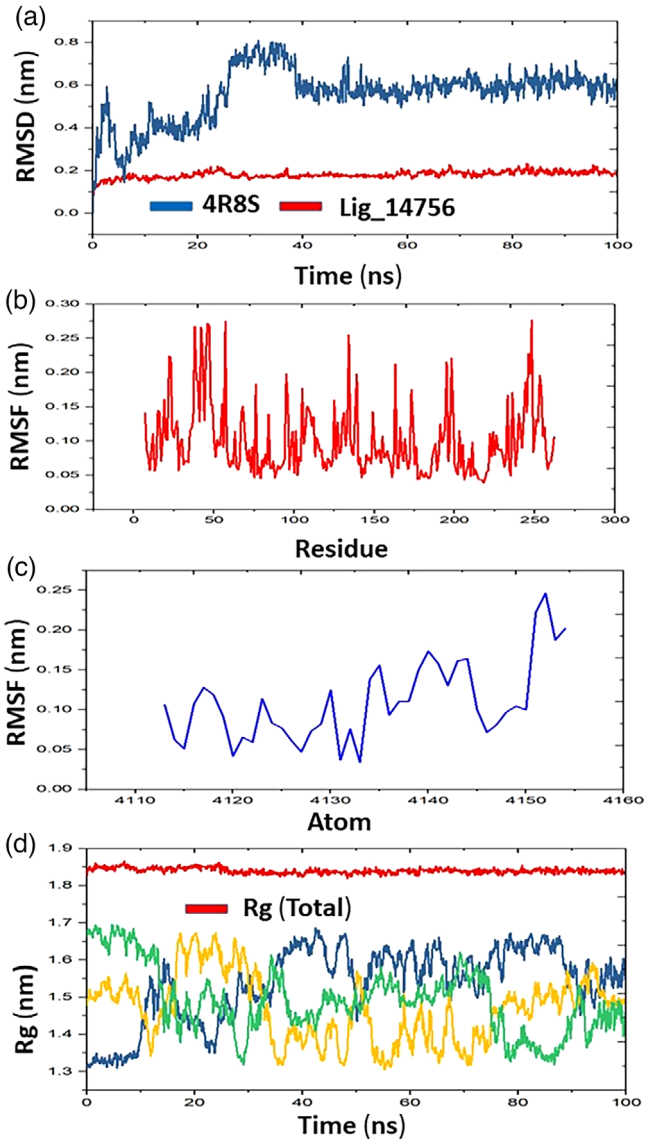

Figure 7. Molecular dynamics trajectory analysis of compound lig_14756_4R8S complex. (a) RMSD, (b) RMSF of protein, (c) RMSF of ligand, and (d) R_g of the complex.

2.2.4. Molecular Dynamics Simulation of lig_CNP0019696-4R8S Complex

The RMSD analysis of the dengue protein 4R8S, illustrated in Figure 11a, reveals a fluctuation range from 0 to 12 nm. Notably, there is an initial heightened fluctuation during the first 20 ns, after which the RMSD stabilizes for the remainder of the simulation period. Concurrently, the RMSD of the ligand maintains stability, ranging between 0.02 and 0.2 nm throughout the entire simulation. Examining the RMSF of the protein (Figure 11b), fluctuations in the range of 0.05–0.25 nm are observed for residues 50, 100, 150, 200, and 250. This variability in RMSF underscores the flexibility of these specific residues, indicative of dynamic interactions with ligand atoms. Similarly, the RMSF of the ligand (Figure 11c) demonstrates fluctuations between 0.05 and 0.25 nm, illustrating the ligand's flexibility in interacting with

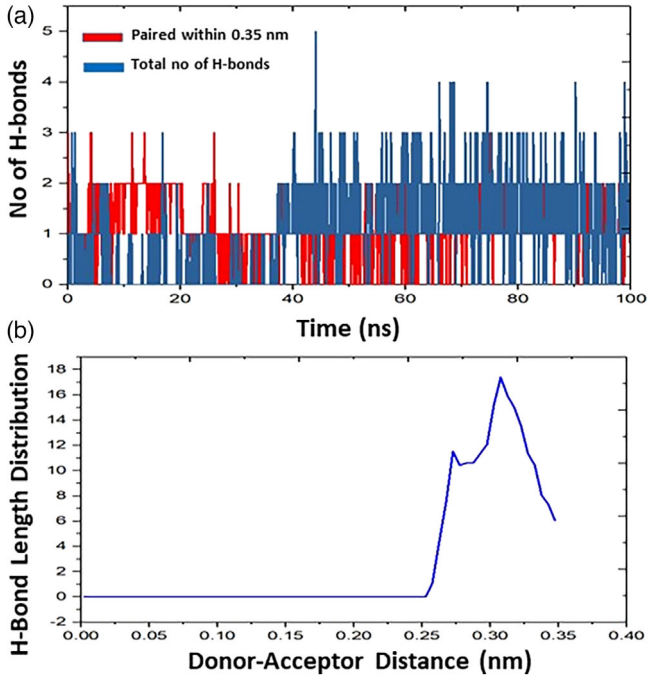

Figure 8. Hydrogen bond trajectory analysis of lig1_14756-4R8S complex. (a) Total number of H bonds and (b) H bond length distributions.

protein residues. Furthermore, the R_g analysis of the complex, as depicted in Figure 11d, indicates a consistent stability of the complex throughout the simulation. These collective findings provide valuable insights into the dynamic behavior, stability, and intermolecular interactions within the studied dengue protein–ligand complex.

Furthermore, an analysis of hydrogen bond distributions was conducted to gain a more profound understanding of the system's stability. As illustrated in Figure 12a,b, the molecule exhibited a substantial number of hydrogen bond distributions throughout the entire 100 ns duration, employing a cutoff value of 0.35 nm. This discovery underscores the heightened stability of the system, indicating a continual presence and maintenance of intermolecular interactions involving hydrogen bonding throughout the simulation.

2.3. Free Energy Landscape Analysis

FEL analysis is a powerful technique used in the study of molecular systems, particularly in the context of understanding the energetics and dynamics of biomolecular processes. Here is a brief overview of FEL analysis in the context of molecular dynamics. The free energy landscape analysis of all the four complex (Figures 13 and 14) revealed that most of the complex showed lowest energy minima showing less number of funnels indicating the stability of complex. The complex of CNP0014493 and CNP0014756 with 4R8S showed minimal number of funnels indicating lowest energy minima in comparison to other two complex indicating the more stable.

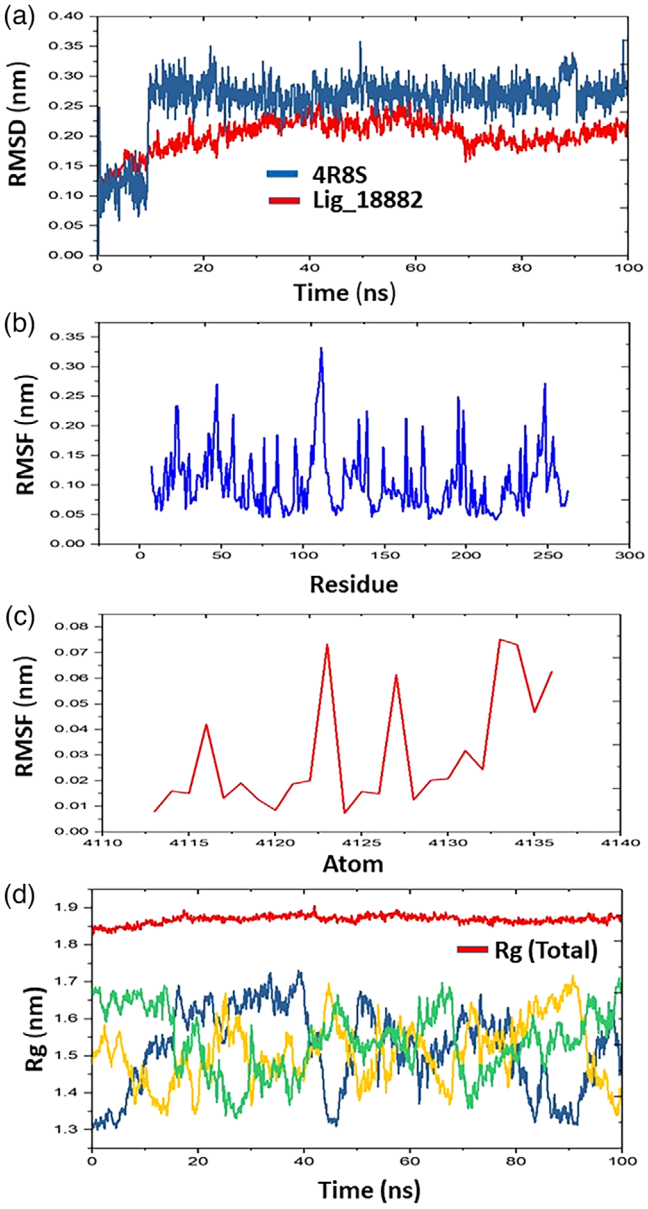

Figure 9. Molecular dynamics trajectory analysis of compound lig_18882_4R8S complex. (a) RMSD, (b) RMSF of protein, (c) RMSF of ligand, and (d) R_g of the complex.

2.4. Binding Free Energy Calculation by MMPBSA

Molecular mechanics Poisson–Boltzmann surface area (MMPBSA) is a computational approach employed to estimate the binding free energy between a ligand and its corresponding protein receptor. Binding free energy calculations using the MMPBSA method were necessary to provide a more accurate and comprehensive assessment of the binding affinity after docking studies.[21] Although docking offers an initial estimation of ligand binding, it does not fully account for solvent effects, conformational flexibility, or entropic contributions. MMPBSA refines these predictions by incorporating these factors, giving a more reliable evaluation of the stability and strength of the interactions between the ligand and the protein.[22] This method

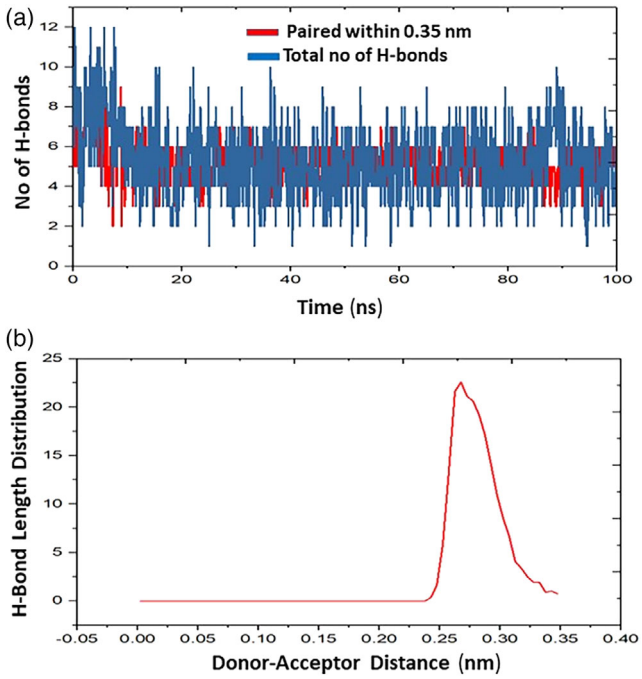

Figure 10. Hydrogen bond trajectory analysis of lig1_18882-4R8S complex. (a) Total number of H bonds and (b) H bond length distributions.

integrates molecular mechanics energies with continuum solvation models to compute the ligand–receptor binding affinity. In our study, binding free energy calculations were performed using the molecular dynamics (MD) trajectories of all complexes to assess their stability. The energy terms considered in these calculations include the van der Waals interactions (VDWAALS), electrostatic energy (EEL), the electrostatic contribution to solvation energy derived from the generalized born (GB) model (EGB), and the nonpolar solvation energy contribution calculated via an empirical model (ESURF). The binding free energy analysis revealed that the complexes CNP0014493 and CNP0014756 exhibited the highest binding energies compared to the other two complexes. The Table S3 showed the binding free energy of all four complex.

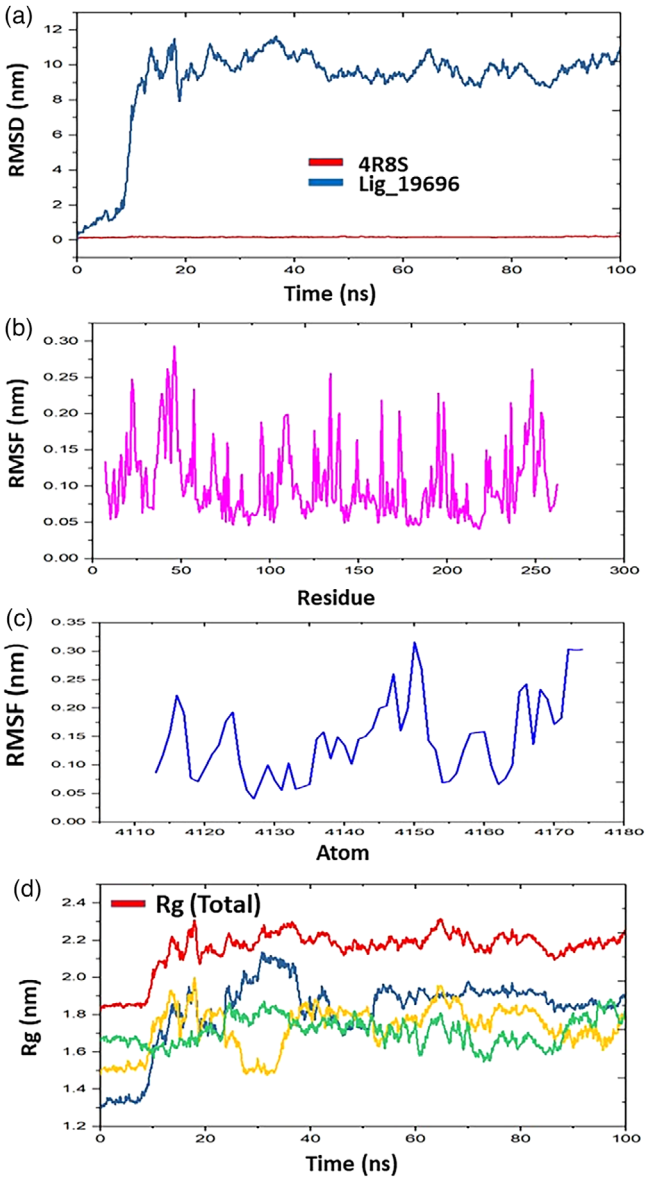

Figure 11. Molecular dynamics trajectory analysis of compound lig_19696_4R8S complex. (a) RMSD, (b) RMSF of protein, (c) RMSF of ligand, (d) R_g of the complex.

2.5. Density Functional Theory

Density functional theory (DFT) is a powerful computational quantum mechanical modelling method widely used in the study of molecular and condensed matter systems, including phytocompounds (bioactive compounds derived from plants).[23] DFT allows researchers to understand the electronic structure of these compounds and predict properties that are relevant in chemistry and biochemistry, such as molecular geometry, reactivity, and interaction with biological targets.[24] So, to better comprehend the chemistry associated with reference compounds, we performed the DFT study of reference compound sinefungin and top hit compound CNP0019696 (selected based on binding score and ADME properties).

2.5.1. Structural Optimization

DFT is widely employed to optimize the geometry of phytocompounds, enabling accurate predictions of bond lengths, bond angles, and dihedral angles. Such information is essential to elucidate the 3D conformation of molecules, which is critical for their interactions with biological targets, including enzymes and receptors. In this study, we optimized the structures of sinefungin and CNP0019696 using the B3LYP functional and the 6-311G(d,p) basis set. Sinefungin comprises 50 atoms and 202 electrons, whereas CNP0019696 consists of 62 atoms and 230 electrons. The optimized structures of both molecules are shown in Figure 15. A summary of the optimized bond lengths

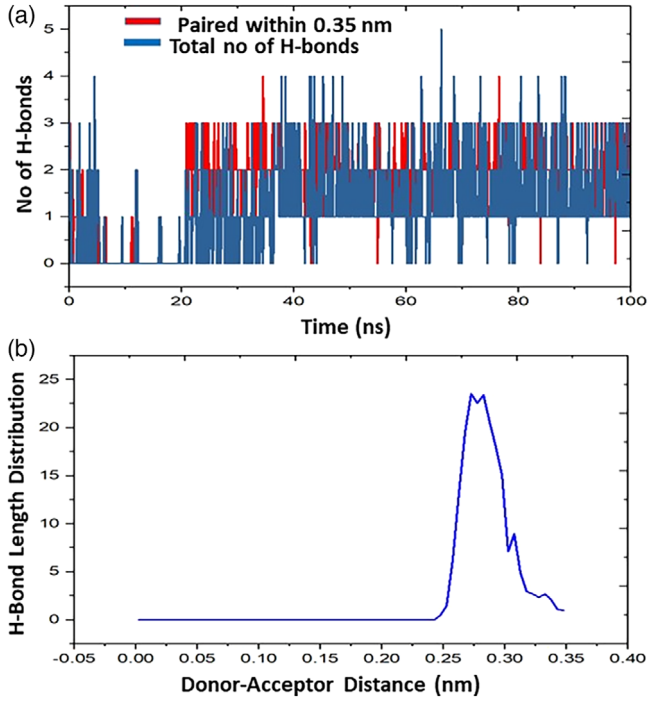

Figure 12. Hydrogen bond trajectory analysis of lig1_19696-4R8S complex. (a) Total number of H bonds and (B) H bond length distributions.

and bond angles for sinefungin and CNP0019696 is provided in Tables S4 and S5, respectively.

2.5.2. Molecular Electrostatic Potential (MEP) Analysis

Molecular electrostatic potential (MEP) is an insightful tool in DFT analysis that provides detailed information regarding the charge distribution within a molecule. Representing the potential energy of a proton at various points in 3D space, MEP arises from the electron density and nuclear positions within the molecule. This visualization reveals the distribution of positive and negative charges, where regions with higher electron density (negative potential) are proton-attracting, whereas regions with lower electron density (positive potential) are proton-repelling. MEP maps are particularly useful for identifying nucleophilic (electron-rich) and electrophilic (electron-poor) regions within a molecule. These maps are typically illustrated as color-coded surfaces overlaid on the molecular geometry, with a gradient—often red for negative potential and blue for positive potential—depicting variations in electrostatic potential. This color gradient allows for an intuitive visualization of reactive sites within the molecule. The MEP map for Compound CNP0019696, shown in Figure 16, highlights regions of electrophilicity and nucleophilicity.

2.5.3. Natural Bond Orbitals (NBO)

HOMO–LUMO gap (highest occupied molecular orbital–lowest unoccupied molecular orbital gap) is a crucial parameter in DFT analysis that provides insight into a molecule's chemical reactivity and stability. A smaller HOMO–LUMO gap suggests higher chemical reactivity as the molecule can more readily accept or donate electrons, making it more reactive and less stable. Conversely, a larger HOMO–LUMO gap indicates greater stability and lower reactivity as the molecule requires more energy for electron excitation. The lower energy gap value for both sinefungin and CNP0019696 was found, which indicated that both the reference compounds are highly reactive (Figure 17). The Global and local reactivity descriptors for reference compound Sinefungin and ligand CNP0019696 were depicted in the Table 1.

Table 1. Global and local reactivity descriptors for title compound sinefungin and ligand CNP0019696.

Parameters	Value (eV)	
	Sinefungin	CNP0019696
E_{HOMO}	−0.23152	−0.20446
E_{LUMO}	−0.03203	−0.00580
Ionization potential	0.23152	0.20446
Electron affinity	0.03203	0.00580
Energy gap (E)	0.19949	0.19866
Electronegativity	0.131775	0.10513
Chemical potential	−0.131775	−0.10513
Chemical hardness	0.099745	0.09933
Chemical softness	10.02	10.06
Electrophilicity index	0.08704	0.05563

2.6. In Silico ADME

In silico ADME (absorption, distribution, metabolism, excretion) studies have become an essential aspect of contemporary drug discovery and development. These computational techniques are utilized to predict the pharmacokinetic behavior of drug candidates within the body, thereby aiding researchers in identifying and optimizing molecules with desirable pharmacokinetic properties at an early stage in the development process. By offering rapid and cost-effective predictions of a compound's potential, in silico ADME studies enhance the efficiency of drug design, minimize the likelihood of failures in later stages of development, and contribute to the creation of safer and more effective therapeutics. In our analysis, all the evaluated molecules demonstrated favorable properties, including an appropriate number of rotatable bonds, hydrogen bond donors and acceptors, Log*P* values, and bioavailability, all of which were consistent with Lipinski's Rule of Five. The Table 2 showed the ADME properties of all four ligands with standard compound sinefungin.

3. Material and Method

3.1. Preparation of Ligand

25,000 molecules were downloaded as Coconut database for phytocompounds[25] for docking study. Before doing the molec-

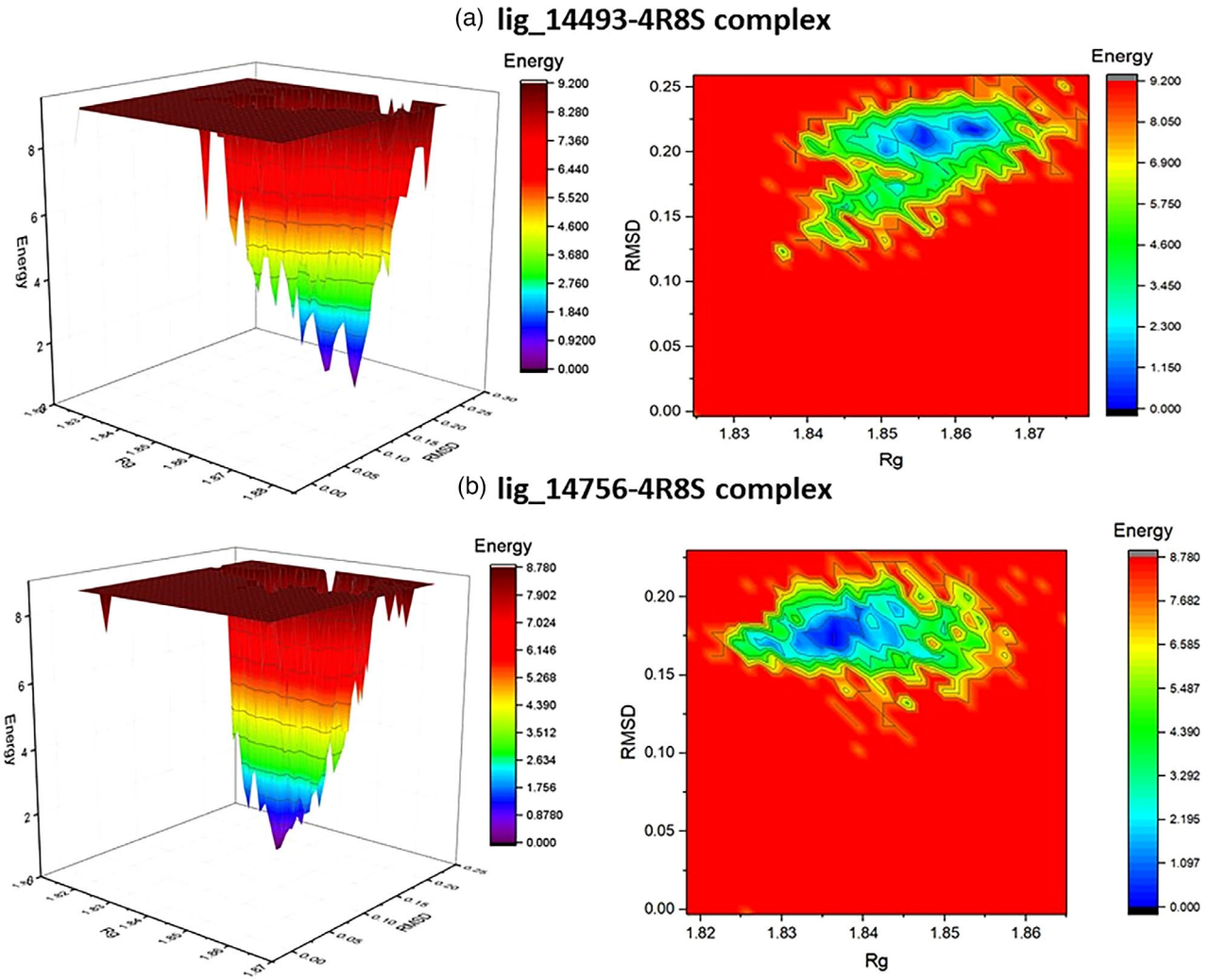

Figure 13. 2D and 3D free energy landscape diagrams illustrate the relationship between the RMSD and RoG for the lig_14493-4R8S and lig_14756-4R8S complexes. Free energy is represented in kilojoules per mole (kJ/mol), with purple indicating regions of minimum energy and red indicating regions of maximum energy.

Table 2. ADME properties of top ten hit molecules using Swiss ADME.

Compound	MW	Rotatable Bonds	H bond Acceptor	H bond Donors	MR	TPSA	ILOGP	XLOGP3	WLOGP	MLOGP	Bioavailability Score	PAINS Alerts	LD_{50} (mg/kg)
Sinefungin	381.39	7	10	6	92.73	208.65	0.67	−4.31	−2.38	−4.72	0.17	0	1000
CNP0018882	474.41	5	11	7	117.63	190.28	1.74	0.93	0.26	−2.01	0.17	0	4400
CNP0019696	429.51	11	6	4	117.57	103.29	3.32	1.97	1.29	0.84	0.55	0	5000
CNP0014493	370.38	5	7	1	99.27	72.5	2.83	1.7	2.16	0.91	0.55	0	300
CNP0014756	340.35	5	5	1	93.63	71.11	1.96	1.51	2.22	1.13	0.55	0	1600

ular docking experiments, this step was performed to optimize the ligand structure in a 3D space. A 3D structure of sinefungine (SNG) was downloaded from the Pubchem database.[26] Chemdraw software was used for geometric and protonation optimization of the ligand.[27] Furthermore, the force field MMFF94 was used for the energy minimization.[28] The SNG was reported as a NS5 MTase inhibitor (IC_{50} = 0.63 μM), used as a control drug for our study. The other screening molecule are collected from Coconut database (reference) and optimized as mention earlier.[16]

3.2. Preparation of Receptor Protein

The 3D structure of the dengue NS5-MTase (PDB ID-4R8S) was downloaded from the RCSB protein data bank. Using the AutoDock tool 1.5.7, the protein structure was optimized.[29]

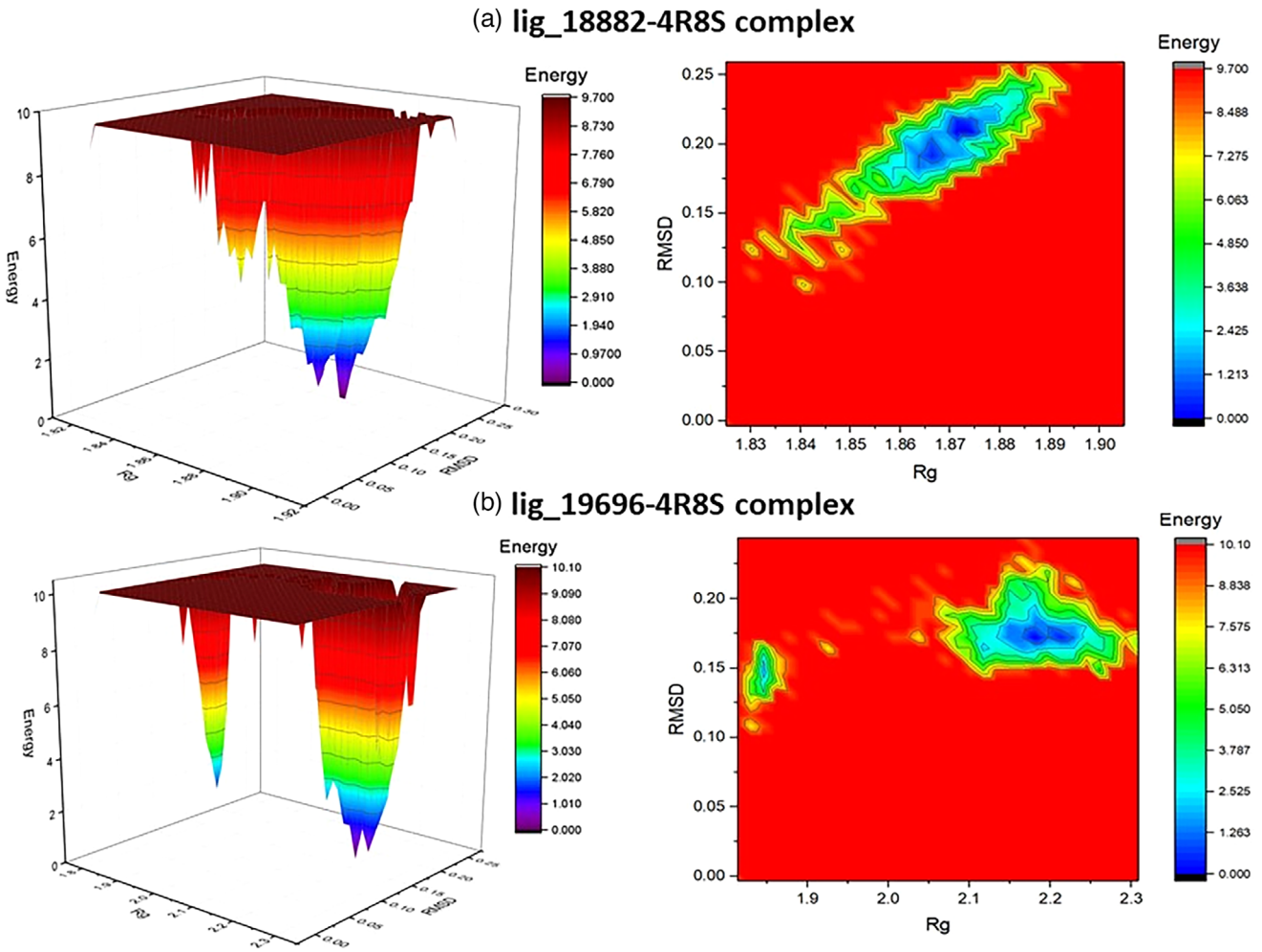

Figure 14. 2D and 3D free energy landscape diagram as a function of RMSD and RoG as the two coordinates of lig_18882-4R8S complex and lig_19696-4R8S. The free energy is displayed in terms of kj/mol where the purple color indicates least energy and red the highest energy.

3.3. Molecular Docking

Molecular docking study was performed by using PyRx Version 0.8.[30] The cocrystal 3D atomic coordinate for the dengue NS5 methyltransferase protein used as standard reference, which is retrieved from the PDB database (PDB ID:4R8S).[31] Firstly, we have performed redock for the cocrystallized ligand for validation of our docking protocol. Exact pose of crystallized ligand matched with our docked pose, with RMSD value 1.478 Å[12]. The docking grid created during docking validation is used for our test molecules. The docking grid dimensions are 52 × 52 × 50 Å, central coordinates X = -10.215; Y = -15.934; Z = 13.166 and 1 Å grid spacing in which almost the entire receptor covered for docking calculations. The receptor was prepared by using PyMol software.[32] Initially all nonstandard atoms and water molecules were removed and the receptor coordinates were retrieved, the Gasteiger charges and polar hydrogens were added and then saved in .pdbqt format by using MGL Tools 1.5.6. (The Scripps Research Institute). The ligand structures were drawn and energy minimized in ChemDraw Ultra 10.0 software. All structures with docking pose visualization and images generated by using (Table 3) Discovery studio visualizer 4.5.[33]

Table 3. Molecular docking parameter as well as PDB IDs of dengue NS5 MTase protein used for molecular docking. RMSD of the best docked poses for each of the crystal structures with respect to their respective crystal structure poses has been provided.

Protein name	PDB ID (Serotype)	Docking Parameter		RMSD (Å)
		Box Dimension X*Y*Z (Å^3)	Docking Box Centre (Å)	
NS5 MTase	4R8S (DENV-3)	52 × 52 × 50	X = −10.215 Y = −15.934 Z = 13.166	1.478

3.4. Molecular Dynamics Simulation

MD simulation is a widely employed computational technique used to examine the physical movements of atoms and molecules. To assess the stability of the docked molecules, we conducted a 100-ns simulation of the docked protein–ligand complex using GROMACS 2020 software. The ligand's best-docked pose was selected to generate the necessary topology files, which were created using the CHARMM-GUI web server's input generator for GROMACS. The server applied the CHARMM

Research Article
doi.org/10.1002/slct.202404185

Chemistry Europe
European Chemical Societies Publishing

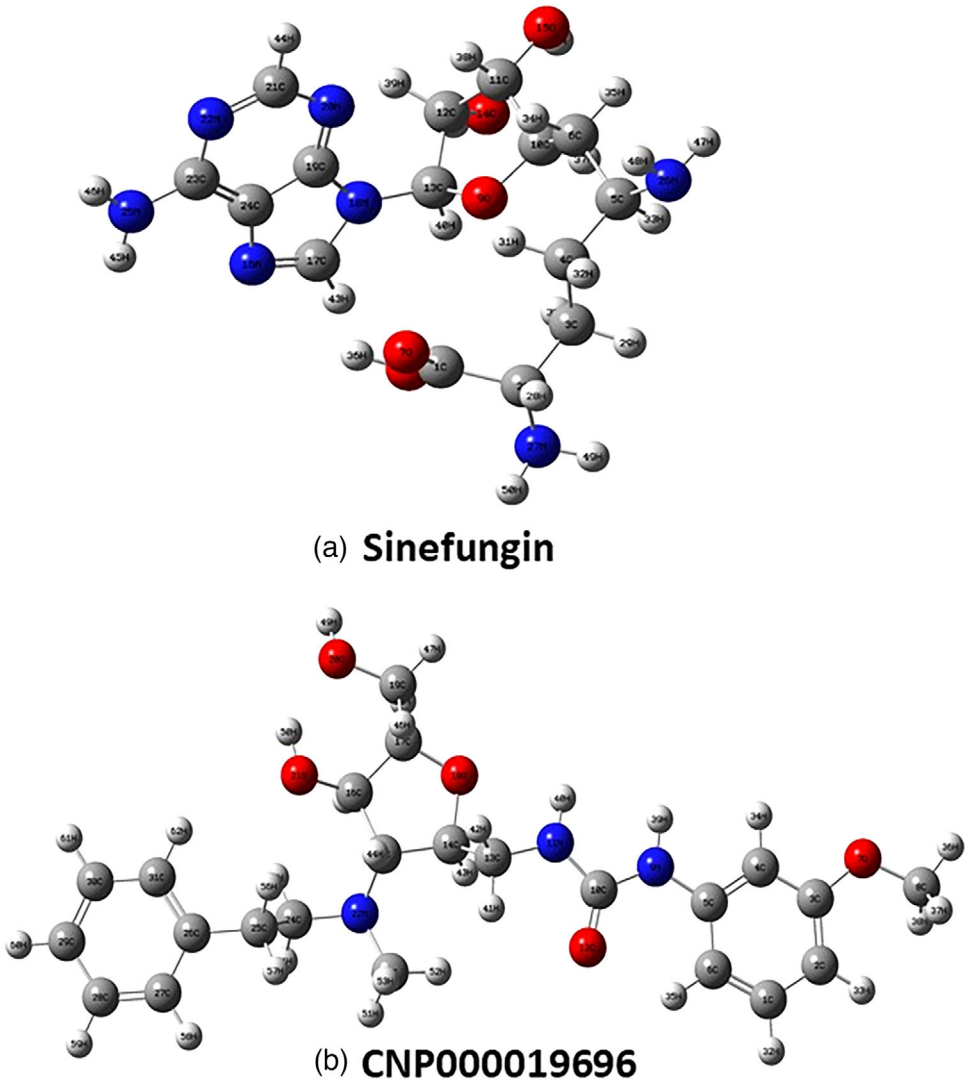

Figure 15. Optimized structure of reference compound (a) sinefungin and (b) hit molecule CNP0019696.

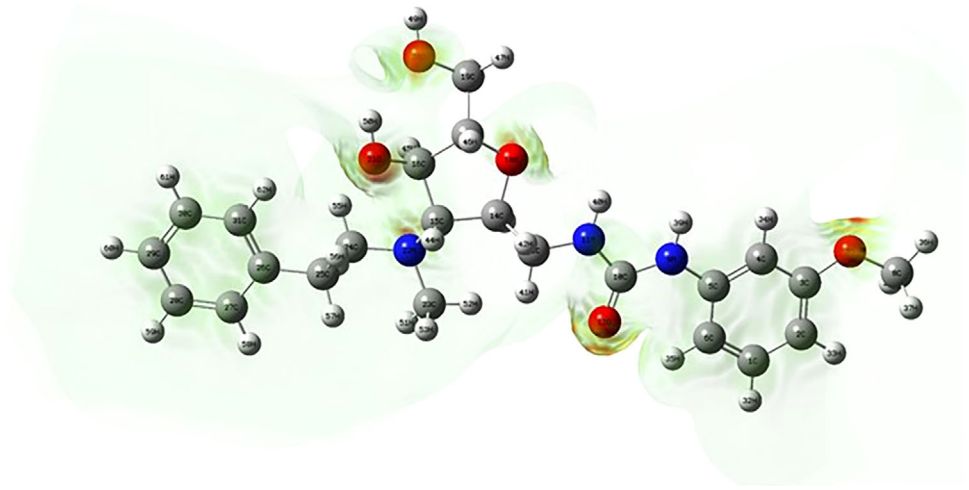

Figure 16. Molecular electrostatic potential (MEP) of compound CNP0019696.

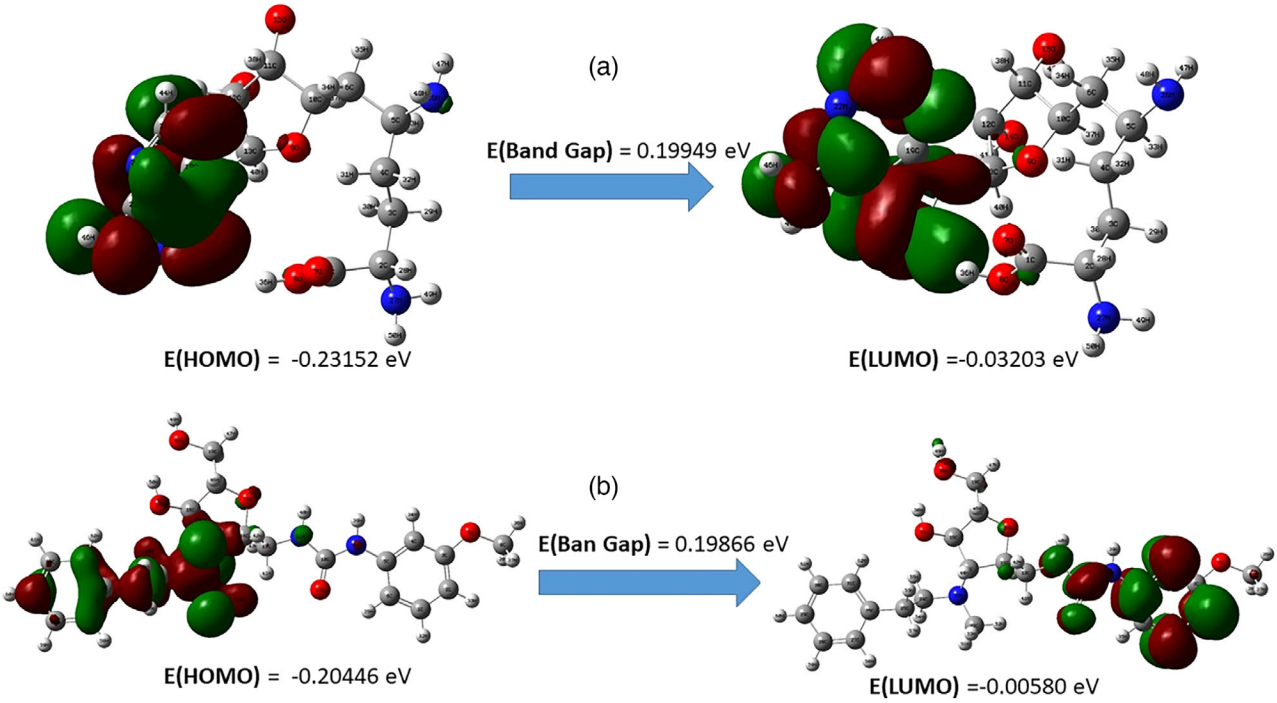

Figure 17. HOMO–LUMO energy diagram of reference compound (a) sinefungin and (b) CNP0019696.

36 m force field to the ligand. This approach is well-documented in the literature.[34,35]

3.5. MMPBSA

The procedure for calculating binding free energy using MMPBSA is thoroughly established in the literature.[35] Prior to performing the calculations with gmx_MMPBSA, periodic boundary conditions were removed, and the GROMACS output trajectory was carefully fitted.[36] In this study, we employed a single-trajectory approach to determine the binding free energy differences.[34]

3.6. Density Functional Theory (DFT)

Density functional theory (DFT) calculations were performed using the B3LYP functional and the 6-311G(d,p)[37,24] basis set with Gaussian software on the CCD cluster at the Computer Department, IIT BHU. B3LYP is one of the most commonly used DFT methods due to its ability to accurately predict molecular structures and various other properties.[24,38]

3.7. In Silico ADME

SwissADME, a web-based platform created by the Swiss Institute of Bioinformatics (SIB), is a widely recognized tool for predicting the ADME characteristics of small molecules.[39,40] It provides a robust set of computational methods to evaluate the drug-likeness and pharmacokinetic properties of potential drug candidates. In this study, the SwissADME tool was utilized via its online portal (http://www.swissadme.ch/) to analyze various properties, including molecular weight (MW), lipophilicity (iLOG*P*), hydrogen bond acceptors (HBA), hydrogen bond donors (HBD), and total polar surface area (TPSA), among other critical parameters.[41] Toxicity dose (LD_{50}) of all four compounds were determined by Protox3 webserver (https://tox.charite.de/protox3/index.php?site = compound_input).

4. Conclusion

Dengue virus is leading cause of mortality affecting millions of people worldwide. In this work we have docked 25,000 molecules from the Coconut database. Structure based virtual screening of 25,000 molecules were performed against NS5 MTase protein. Four molecules were selected based on their top binding affinity and binding patter with the protein residues. Further to better comprehend the binding interaction of top molecules we performed the molecular dynamic simulation of top four complex. All the molecules showed CNP001882, CNP0019696, CNP0014493, and CNP0014756 stable conformation with the protein. Further, free energy landscape suggested that all the molecules showed lowest energy minima showing the stability of complex. Binding energy calculation demonstrated that the molecules CNP0014493, and CNP0014756 showed good binding affinity compared to other ligands. Further DFT study revealed that the reference compound, as well as the top identified ligand CNP0019696, displayed promising stability and electronic properties favorable for binding interactions. Analysis of the HOMO–LUMO energy gap showed that both compounds possess an optimal balance between stability and reactivity,

which is essential for effective molecular recognition. Further, in silico ADME study revealed the favorable pharmacokinetic properties of all four ligands along with reference compound.

Acknowledgements

Dr. Bhanuranjan Das is grateful to the Indian Institute of Technology (BHU), Institutional fellowship, provided during his teaching assistantship. Mr. Purna Chandra Pal thanks for the resource provide by Department of Pharmaceutical technology, Brainware University. The support and the resources provided by "PARAM Shivay Facility" under the National Supercomputing Mission, Government of India, at the Indian Institute of Technology (BHU), Varanasi, are gratefully acknowledged.

Conflict of Interests

The authors declare no conflict of interest.

Data Availability Statement

The data that support the findings of this study are available in the Supporting Information of this article.

Keywords: Dengue · DFT · MM-PBSA · Molecular docking · Molecular dynamics

[1] WHO Organization, Comprehensive Guideline for Prevention and Control of Dengue and Dengue Haemorrhagic Fever **2011**.
[2] R. Dehghani, H. Kassiri, *Res. J. Pharm. Technol.* **2021**, *14*, 2296–2301.
[3] V. H. Ferreira-de-Lima, T. N. Lima-Camara, *Parasites Vectors* **2018**, *11*, 1–8.
[4] R. Rodriguez-Roche, E. A. Gould, *Biomed Res. Int.* **2013**, *2013*, 690835.
[5] G. N. Malavige, P. Sjö, K. Singh, J.-M. Piedagnel, C. Mowbray, S. Estani, S. C. L. Lim, A. M. Siquierra, G. S. Ogg, L. Fraisse, *PLOS Glob. Public Health* **2023**, *3*, e0002598.
[6] P. Biswas, S. Ganguly, B. Debnath, *Asian J. Pharm. Clin. Res.* **2021**, *14*, 3–11.
[7] G. Andrei, *Front. Media SA* **2021**, *1*, 666548.
[8] V. C. Maddipati, L. Mittal, M. Mantipally, S. Asthana, S. Bhattacharyya, R. Gundla, *Curr. Pharm. Des.* **2020**, *26*, 4386–4409.
[9] D. Madhry, K. K. Pandey, J. Kaur, Y. Rawat, L. Sapra, R. Kumar, R. K. Srivastava, S. Bhattacharyya, B. Verma, *Front. Biosci. Sch.* **2021**, *13*, 44–55.
[10] A. Murugesan, M. Manoharan, in *Emerging and Reemerging Viral Pathogens*, Elsevier, Amsterdam, Netherlands **2020**, pp. 281–359.
[11] N. Uno, T. M. Ross, *Emerg. Microbes Infect.* **2018**, *7*, 1–11.
[12] L. M. Higa, B. M. Curi, R. S. Aguiar, C. C. Cardoso, A. G. De Lorenzi, S. L. Sena, R. B. Zingali, A. T. Da Poian, *PLoS One* **2014**, *9*, e88314.
[13] M. Bollati, K. Alvarez, R. Assenberg, C. Baronti, B. Canard, S. Cook, B. Coutard, E. Decroly, X. de Lamballerie, E. A. Gould, *Antiviral Res.* **2010**, *87*, 125–148.
[14] Y. Zhou, D. Ray, Y. Zhao, H. Dong, S. Ren, Z. Li, Y. Guo, K. A. Bernard, P.-Y. Shi, H. Li, *J. Virol.* **2007**, *81*, 3891–3903.
[15] S. Idrus, U. S. F. Tambunan, A. A. Zubaidi, *Bioinformation* **2012**, *8*, 348.
[16] M. Sorokina, P. Merseburger, K. Rajan, M. A. Yirik, C. Steinbeck, *J. Cheminform.* **2021**, *13*, 2.
[17] B. Selisko, F. F. Peyrane, B. Canard, K. Alvarez, E. Decroly, *J. Gen. Virol.* **2010**, *91*, 112–121.
[18] X.-C. Cai, K. Kapilashrami, M. Luo, in *Methods in Enzymology*, Elsevier Amsterdam, Netherlands **2016**, pp. 245–308.
[19] R. Ahmed-Belkacem, P. Sutto-Ortiz, M. Guiraud, B. Canard, J.-J. Vasseur, E. Decroly, F. Debart, *Eur. J. Med. Chem.* **2020**, *201*, 112557.
[20] E. W. Bell, Y. Zhang, *J. Cheminf.* **2019**, *11*, 1–9.
[21] E. Wang, H. Sun, J. Wang, Z. Wang, H. Liu, J. Z. Zhang, T. Hou, **2019**, *Chem. Rev.*, *119*, 9478–9508.
[22] G. Rastelli, A. D. Rio, G. Degliesposti, M. Sgobba, *J. Comput. Chem.* **2010**, *31*, 797–810.
[23] S. Saha, P. Biswas, M. I. Tareq, M. Rahman Sakib, S. Akter Rakhi, M. N. H. Zilani, A. H. Harrath, M. A. Rahman, M. N. Hasan, *Appl. Sci.* **2024**, *14*, 9878.
[24] B. Das, A. T. Baidya, B. Devi, T. Rom, A. K. Paul, B. Thakur, T. Darreh-Shori, R. Kumar, *J. Mol. Struct.* **2023**, *1276*, 134782.
[25] D. L. Sheela, P. A. Nazeem, A. Narayanankutty, R. M. Shylaja, S. P. Davis, P. James, R. Valsalan, T. D. Babu, A. C. Raghavamenon, *Prostagland. Leukotrienes Essent. Fatty Acids* **2017**, *127* 20–24.
[26] S. Kim, J. Chen, T. Cheng, A. Gindulyte, J. He, S. He, Q. Li, B. A. Shoemaker, P. A. Thiessen, B. Yu, *Nucleic Acids Res.* **2023**, *51*, D1373–D1380.
[27] N. Mills, *J. Am. Chem. Soc.* **2006**, *128*, 13649–13650.
[28] T. A. Halgren, *J. Comput. Chem.* **1996**, *17*, 490–519.
[29] P. Sapjaroen, P. Tangyuenyongwatana, in The 35th International Annual Meeting in Pharmaceutical Sciences & CU-MPU International Collaborative Research Conference Study, Bangkok, Thailand **2019**, pp. 155–158.
[30] U. Ounthaisong, P. Tangyuenyongwatana, *TJPS* **2017**, *41*, 189–192.
[31] C. G. Noble, S.-H. Li, H. Dong, S. H. Chew, P.-Y. Shi, *Antiviral Res.* **2014**, *111*, 78–81.
[32] D. Seeliger, B. L. de Groot, *J. Comput.-Aided Mol. Des.* **2010**, *24*, 417–422.
[33] D. Studio, Discovery studio 2008, Accelrys [2.1], 420.
[34] B. Das, A. T. Mathew, A. T. Baidya, B. Devi, R. R. Salmon, R. Kumar, *Mol. Divers.* **2023**, *28*, 2013–2031.
[35] A. T. Baidya, B. Das, B. Devi, B. Långström, H. Ågren, T. Darreh-Shori, R. Kumar, *ACS Chem. Neurosci.* **2023**, *14*, 749–765.
[36] M. S. Valdés-Tresanco, M. E. Valdés-Tresanco, P. A. Valiente, E. Moreno, *J. Chem. Theory Comput.* **2021**, *17*, 6281–6291.
[37] J. Tirado-Rives, W. L. Jorgensen, *J. Chem. Theory Comput.* **2008**, *4*, 297–306.
[38] B. Das, A. T. Baidya, S. Chakrabarti, D. Chouhan, B. Thakur, T. Darreh-Shori, G. Chen, V. Tiwari, R. Kumar, *Bioorg. Chem.* **2024**. *147*, 107373.
[39] M. Mahanthesh, D. Ranjith, R. Yaligar, R. Jyothi, G. Narappa, M. Ravi, *J. Pharmacogn. Phytochem.* **2020**, *9*, 1799–1809.
[40] S. Kar, J. Leszczynski, *Expert Opin. Drug Discov.* **2020**, *15* 1473–1487.
[41] B. Das, A. T. Mathew, A. T. Baidya, B. Devi, R. R. Salmon, R. Kumar, *Mol. Divers.* **2024**, *28*, 2013–2031.

Manuscript received: September 1, 2024